

## EFFECT OF SiO<sub>2</sub> COATING ON MICROSTRUCTURE AND DIELECTRIC PROPERTIES OF BaZr<sub>0.1</sub>Fe<sub>0.02</sub>Ti<sub>0.88</sub>O<sub>3</sub> CERAMICS

Z. LI<sup>a,b,\*</sup>, Y. LI<sup>c</sup>, H. ZHOU<sup>a</sup>, Z. WANG<sup>a</sup>

<sup>a</sup>Chemical College, Shijiazhuang University, Shijiazhuang 050035, China

<sup>b</sup>Hebei Building Ceramics Engineering Research Centre, Shijiazhuang 050035, China

<sup>c</sup>Analysis and Testing Research Centre, North China University of Science and Technology, Tangshan 063210, China

BaCO<sub>3</sub>, ZrO<sub>2</sub>, TiO<sub>2</sub> and Fe<sub>2</sub>O<sub>3</sub>, were used as the starting materials, the BaZr<sub>0.1</sub>Fe<sub>0.02</sub>Ti<sub>0.88</sub>O<sub>3</sub> powders are prepared using solid state synthesis method, the powders were coated with SiO<sub>2</sub>, the influence of different SiO<sub>2</sub> package on the structure, micro morphology and dielectric properties of the samples is studied. The results show that all the samples have typical diffraction peaks of perovskite crystal; however, with the increase of the amount of inclusion of SiO<sub>2</sub>, a part of SiO<sub>2</sub> enters into the crystal lattice, forming the BaTiSi<sub>4</sub>O<sub>11</sub> phase in the body. The grain size of the sample coated with SiO<sub>2</sub> is significantly larger than that of the sample not coated, with the continuous increase of the amount of coating, the grain size has no obvious change, and the size distribution is relatively uneven. With the increase of SiO<sub>2</sub> content, the dielectric constant of the sample increases first and then decreases, and the dielectric loss of the sample decreases first and then increases. Due to the coating of SiO<sub>2</sub>, the dielectric constant is 2736, and the dielectric loss is 0.033 when the content of SiO<sub>2</sub> is 1 wt%.

(Received January 13, 2020; Accepted May 11, 2020)

*Keywords:* Ceramics, Microstructure, Dielectric properties, Coating

### 1. Introduction

With the depletion of petroleum energy, electric vehicles emerge as the times require. At present, the batteries used in electric vehicles have small storage capacity and serious environmental pollution [1-3]. The electric energy storage unit (EESU) made of high dielectric constant and modified BaTiO<sub>3</sub> ceramic powder is characterized by high safety index, short charge discharge time, high energy density and long service life [4-6]. BaTiO<sub>3</sub> with excellent dielectric properties has been widely used in ceramic capacitors, but pure BaTiO<sub>3</sub> has low breakdown voltage, strong dielectric nonlinearity, and is difficult to maintain large capacitance, which limits its application in the field of energy storage. According to the formula (1),

$$E = \frac{1}{2} CV^2 \quad (1)$$

where  $E$  is the energy,  $C$  is the capacitance, and  $V$  is the applied voltage of sample. It is important to improve the breakdown voltage and dielectric constant of BaTiO<sub>3</sub> and reduce the dielectric nonlinearity for the development of BaTiO<sub>3</sub> based energy storage capacitor [7].

The dielectric constant of barium zirconate titanate ceramics is high near room temperature, and the dielectric properties of ceramics are stable in high temperature DC electric field and reduction atmosphere. However, in the AC electric field, the free charge accumulates at the grain boundary, increasing the dielectric loss of the material; when the free charge accumulates to a certain extent, it is easy to be broken down under high voltage. BaTi<sub>1-x</sub>Zr<sub>x</sub>O<sub>3</sub>-based dielectric ceramics have high dielectric constant, which makes it possible to manufacture ceramic capacitors [8,9]. However, its dielectric strength and dielectric loss need to be improved Material

---

\* Corresponding author: midfall@aliyun.com

modification can be realized by doping and coating. Many researchers have done some research on surface coating modification and made a lot of progress [10,11]. Fang, et al [12], have used sol-gel method to prepare  $(\text{Ba}_{0.97}\text{La}_{0.02})(\text{Ti}_{0.97}\text{Fe}_{0.04})\text{O}_3$  sol coated  $\text{BaTiO}_3$  nanopowders by different sintering processes. After coating the powder with sol, a thin wrapping layer was formed around the powder. The existence of the coating makes the  $\text{BaTiO}_3$  grains subject to large internal stress, and the size distribution of the ceramic particles is relatively uniform. The Curie temperature moves with the increase of the dielectric constant, and the peak value of the Curie point widens with the decrease of the grain size. Jae [13] et, al, have prepared  $\text{BaTiO}_3$  powder coated with  $\text{MgO}$  by homogeneous precipitation method. The dielectric constant of  $\text{BaTiO}_3$  powders doped with  $\text{MgO}$  decreases with the increase of  $\text{MgO}$  content, while the dielectric constant of  $\text{BaTiO}_3$  powders coated with  $\text{MgO}$  shows a low dependence on  $\text{MgO}$  content, which may be caused by different "core-shell" structure and  $\text{Mg}^{2+}$  replacing  $\text{Ti}^{4+}$ . In this paper,  $\text{BaZr}_{0.1}\text{Ti}_{0.9}\text{O}_3$  is the main crystal phase, and  $\text{Fe}_2\text{O}_3$  with a certain mole percentage is doped. The influence of different  $\text{SiO}_2$  package on the structure, micro morphology, dielectric properties and dielectric temperature spectrum characteristics of the samples is studied.

## 2. Experimental

The formula of the ceramics studied was  $\text{BaZr}_{0.1}\text{Fe}_{0.02}\text{Ti}_{0.88}\text{O}_3$  (BZFT). The samples were prepared by the two-stage method to acquire a pure phase of perovskite. Reagent-grade oxide powders,  $\text{BaCO}_3$ ,  $\text{ZrO}_2$ ,  $\text{TiO}_2$  and  $\text{Fe}_2\text{O}_3$ , were used as the starting materials. At first, a powder of  $\text{BaZr}_{0.1}\text{Fe}_{0.02}\text{Ti}_{0.88}\text{O}_3$ , was prepared by calcination of  $\text{BaCO}_3$ ,  $\text{ZrO}_2$ ,  $\text{TiO}_2$  and  $\text{Fe}_2\text{O}_3$ , at  $1050\text{ }^\circ\text{C}$  for 2 h. Secondly, TEOS and ETOH were mixed in a certain proportion, and then placed in a cold water bath, stirred for 10 min. Add the mixture of nitric acid and water drop by drop under the magnetic stirrer, and adjust the pH to about 2. Then continue to stir until the solution reaches the sol state, ready for use. Thirdly, weigh a certain amount of  $\text{BaZr}_{0.1}\text{Fe}_{0.02}\text{Ti}_{0.88}\text{O}_3$  powder and put it into the beaker, add a proper amount of ETOH as the dispersant, and make the powder fully disperse under the effect of magnetic stirring. The slurry is drained into a beaker in the sol state with a glass rod and stirred for 30 min to make them fully wrapped. Then the liquid is dried in an oven at a temperature of about  $65\text{ }^\circ\text{C}$ . After calcining the dried powder at  $850\text{ }^\circ\text{C}$  and cooling with the furnace, the BZFT ceramic powder coated with  $\text{SiO}_2$  was obtained. The above precursor granulated (with polyvinyl alcohol as binder), pressed into the desired form ( $\Phi \times d = 12.00 \times 2.00\text{ mm}^2$ ) at 10 Mpa, and then sintered at  $1250\text{ }^\circ\text{C}$ ,  $1280\text{ }^\circ\text{C}$ ,  $1300\text{ }^\circ\text{C}$  and  $1330\text{ }^\circ\text{C}$  for 2 h in the air, respectively. The sintered samples were cleaned using an ultrasonic bath, then dried. Both sides of the specimens for dielectric property measurements were screened electrode paste composing mainly of  $\text{AgO}$ , some fluxes and binders, then fired at  $650\text{ }^\circ\text{C}$  for 10 min.

The crystal structure of the samples was detected using X-ray diffraction (XRD, Model RIGAKU D/MAX 2500V/PC, Japan) characterization with a  $2\theta$  range from  $10^\circ$  to  $70^\circ$ . The micrographs of the samples were observed by field emission scanning electron microscopy (SEM, Hitachi s4800). Room-temperature dielectric constant and dielectric loss were measured using an LCR meter (Model YY 281 automatic LCR Meter 4225). The temperature dependence of the dielectric constant ( $\epsilon$ ) was measured using a capacitance apparatus (Model YY 281 automatic LCR Meter 4225) at 1 kHz in a temperature range over  $25\text{ }^\circ\text{C}$  to  $125\text{ }^\circ\text{C}$ .

## 3. Results and discussions

Under the condition of  $1300\text{ }^\circ\text{C}$  sintered for 2 h, the XRD results of the sample are shown in Fig. 1. It can be seen from Fig.1 that all the samples have typical diffraction peaks of perovskite crystal, that is, the inclusion does not cause the change of the main crystal phase. With the increase of the amount of inclusion of  $\text{SiO}_2$ ,  $\text{BaTiSi}_4\text{O}_{11}$  phase appears between (100) and (110) crystal planes, indicating that the inclusion of  $\text{SiO}_2$  does not only exist on the surface of the system, but also a part of  $\text{SiO}_2$  enters into the crystal lattice, forming other crystal phases in the body. When

the amount of inclusions is less than 1 wt%, the diffraction peak moves towards the smaller angle direction, when the amount of inclusions is 1wt%, the angle of  $2\theta$  reaches the minimum, when the amount of inclusions is more than 1 wt%, the diffraction peak moves towards the large angle direction. According to the bragg equation, when the amount of inclusions is less than 1 wt%, the crystal surface spacing increases with the increase of the amount of inclusions. When the amount of inclusions is more than 1 wt%, the crystal surface spacing decreases with the increase of the amount of inclusions, that is, when the amount of inclusions is 1 wt%, the crystal surface spacing reaches the maximum.

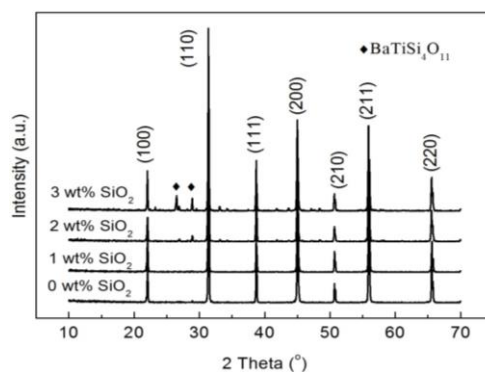


Fig. 1. XRD patterns of BZFT ceramics with different package quantity of  $\text{SiO}_2$ .

Under the condition of sintered at  $1300\text{ }^\circ\text{C}$  for 2 h, SEM micrographs of the surface is shown in Fig. 2. It can be seen from Fig.2 that the grain size of the sample coated with  $\text{SiO}_2$  is significantly larger than that of the sample not coated. With the continuous increase of the amount of coating, the grain size has no obvious change, and the size distribution is relatively uneven, showing an irregular ellipse. It can be seen that  $\text{SiO}_2$  inclusions can promote the growth of grains, but when the amount of  $\text{SiO}_2$  inclusions increases to a certain amount, the effect of promoting grains will be weakened. It can also be seen that the porosity is the smallest and the density is the best when the package content is 1wt%. The corresponding bulk density curve is shown in Fig. 3, that is, with the increase of  $\text{SiO}_2$  content in the system, the densification first increases and then decreases. When the content is 1 wt%, the densification is the highest, which is basically consistent with the analysis results of SEM.

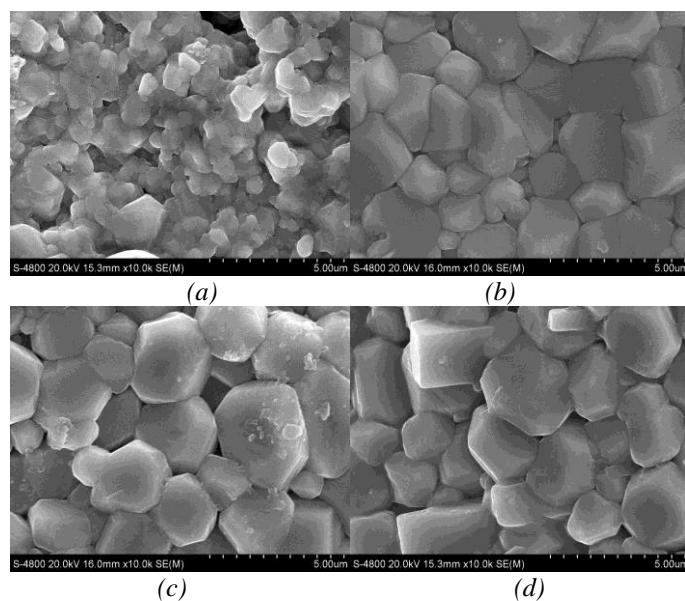


Fig. 2. SEM micrographs of the surface of BZFT ceramics with different package quantity of  $\text{SiO}_2$ .  
(a) 0 wt%; (b) 1 wt%; (c) 2 wt%; (d) 3 wt%

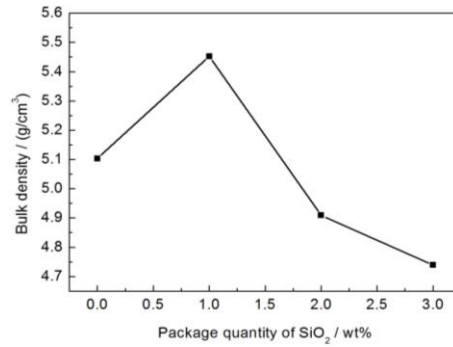


Fig. 3. Bulk density of the BZFT ceramics with different package quantity of SiO<sub>2</sub>.

Under the conditions of sintered at 1250 °C, 1280 °C, 1300 °C and 1330 °C for 2 h, respectively, the change of dielectric constant  $\epsilon_r$  with the package amount of SiO<sub>2</sub> is shown in Fig. 4. It can be seen from Fig. 4 that at room temperature, with the increase of SiO<sub>2</sub> content, the dielectric constant of the sample increases first and then decreases. When the content of SiO<sub>2</sub> is 1 wt%, the dielectric constant of the system is the largest, and the dielectric constant is 2736. The decrease of dielectric constant may be due to the formation of capacitors with grain boundary layer when package quantity of SiO<sub>2</sub> is more than 1 wt%, a large number of oxygen vacancies were formed after the coating of SiO<sub>2</sub> [14]. The oxygen vacancies were segregated near the BZFT and the insulating grain boundary, which led to the strengthening of space charge polarization and the formation of grain boundary effect. Because the dielectric properties of grain boundary layer ceramic capacitor mainly depend on its unique core-shell structure, According to the formula (2) of dielectric constant of grain boundary layer capacitor ,

$$\epsilon_r = \frac{d_g}{d_b} \epsilon_b \quad (2)$$

where,  $d_g$  is the grain size,  $d_b$  is the thickness of the grain boundary insulation, and  $\epsilon_b$  is dielectric constant of the grain boundary insulating layer. Obviously, the thinner the grain boundary is, the higher the dielectric constant is [15]. With the increase of SiO<sub>2</sub> content, the thickness of the grain boundary insulation becomes more large, then dielectric constant decreases.

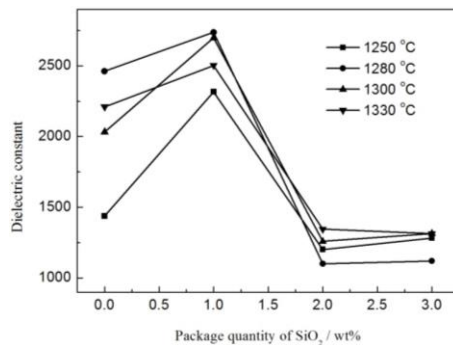


Fig. 4. Dielectric constant of the BZFT ceramics with different package quantity of SiO<sub>2</sub>.

Under the conditions of sintered at 1250 °C, 1280 °C, 1300 °C and 1330 °C for 2 h, respectively, the change of dielectric loss with the package amount of SiO<sub>2</sub> is shown in Fig. 5. It can be seen from Fig. 5 that at room temperature, with the increase of SiO<sub>2</sub> content, the dielectric loss of the sample decreases first and then increases. When the content of SiO<sub>2</sub> is 1 wt%, the dielectric loss of the system is the smallest, and the dielectric loss is 0.033. It is difficult to form liquid phase and fill the gap between particles when SiO<sub>2</sub> is calcined at high temperature.

Therefore, the dielectric loss is increase when package quantity of  $\text{SiO}_2$  is more than 1 wt%, which is consistent with the results from Fig. 3.

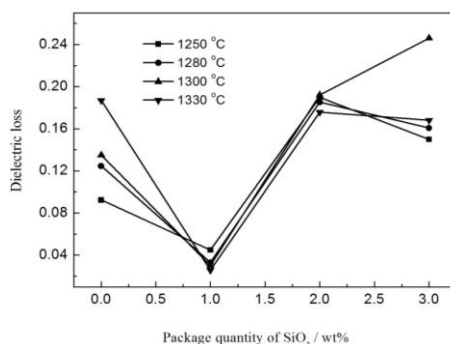


Fig. 5. Dielectric loss of the BZFT ceramics with different package quantity of  $\text{SiO}_2$ .

Under the condition of sintered at 1300 °C for 2 h, the change of the dielectric constant of the sample with the temperature is shown in Fig. 6. It can be seen from Fig. 6 that the dielectric constant of the Curie peak of the sample increases significantly when the amount of  $\text{SiO}_2$  is 1 wt%, and it has a significant broadening effect on the Curie peak. With the increase of the amount of inclusion, the dielectric constant peak begins to decrease. Therefore, it can be concluded that the dielectric property of the sample is the best when the package quantity of  $\text{SiO}_2$  is 1 wt%.

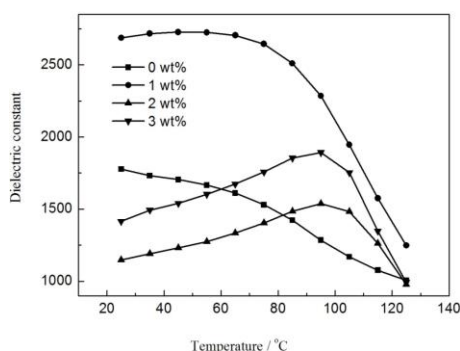


Fig. 6. Temperature dependence of dielectric constants of the BZFT ceramics with different package quantity of  $\text{SiO}_2$ .

#### 4. Conclusions

Using  $\text{BaCO}_3$ ,  $\text{ZrO}_2$ ,  $\text{TiO}_2$  and  $\text{Fe}_2\text{O}_3$  as the starting materials, the  $\text{BaZr}_{0.1}\text{Fe}_{0.02}\text{Ti}_{0.88}\text{O}_3$  powders are prepared using solid state synthesis method, the powders were coated with  $\text{SiO}_2$ , the influence of different  $\text{SiO}_2$  package on the structure, micro morphology and dielectric properties of the samples is also studied. All the samples have typical diffraction peaks of perovskite crystal, however, with the increase of the amount of inclusion of  $\text{SiO}_2$ ,  $\text{BaTiSi}_4\text{O}_{11}$  phase appears between (100) and (110) crystal planes, indicating that the inclusion of  $\text{SiO}_2$  does not only exist on the surface of the system, but also a part of  $\text{SiO}_2$  enters into the crystal lattice, forming other crystal phases in the body. The grain size of the sample coated with  $\text{SiO}_2$  is significantly larger than that of the sample not coated, with the continuous increase of the amount of  $\text{SiO}_2$  coating, the grain size has no obvious change. With the increase of  $\text{SiO}_2$  content, due to the coating of  $\text{SiO}_2$ , the dielectric constant reaches the maximum 2736, and the dielectric loss reaches the minimum 0.033 when the content of  $\text{SiO}_2$  is 1 wt%. The decrease of dielectric constant may be due to the formation of capacitors with grain boundary layer when package quantity of  $\text{SiO}_2$  is more than 1 wt%, with the

increase of SiO<sub>2</sub> content, the thickness of the grain boundary insulation becomes more large, then dielectric constant decreases.

### Acknowledgements

This work was financially supported by the Scientific Research Projects of Hebei Building Ceramics Engineering Research Centre and the Scientific Research Projects of Colleges and Universities in Hebei Province (Grant No. Z2014112), P. R. China.

### References

- [1] L. P. Yao, Q. Zeng, T. Qi et al., *Journal of Cleaner Production* **245**, 118820 (2020).
- [2] C. Li, Z. N. Zhu, Y. M. Wang et al., *Nano Energy* **69**, 104380 (2020).
- [3] B. Huang, Z. F. Pan, X. Y. Su et al., *Journal of Power Sources* **399**, 274 (2018).
- [4] J. C. Wang, Y. Sun, P. N. Wang et al., *Journal of Alloys and Compounds* **789**, 785 (2019).
- [5] M. Wei, J. H. Zhang, M. M. Zhang et al., *Ceramics International* **43**, 4768 (2017).
- [6] K. Bi, M. H. Bi, Y. N. Hao et al., *Nano Energy* **51**, 513 (2018).
- [7] D. Zhang, Z. Wu, X. F. Zhou et al., *Sensors and Actuators A: Physical* **260**, 228 (2017).
- [8] M. Deluca, C. A. Vasilescu, A. C. Ianculescu et al., *Journal of the European Ceramic Society* **32**, 3551 (2012).
- [9] Q. Li, R. Zhang, T. Q. Lv et al., *Ceramics International* **41**, 6560 (2015).
- [10] J. S. Park, Y. H. Han, *Ceramics International* **32**, 673 (2006).
- [11] M. Cernea, B. S. Vasile, A. Boni et al., *Journal of Alloys and Compounds* **587**, 553 (2014).
- [12] L. M. Fang, Y. Shao, F. Zhang, *China Ceramic Industry* **16**, 6 (2009).
- [13] J. S. Park, M. H. Yang, Y. H. Han, *Materials Chemistry and Physics* **104**, 261 (2007).
- [14] F. Bian, S. G. Yan, C. H. Xu et al., *Journal of the European Ceramic Society* **38**, 3170 (2018).
- [15] M. Q. Shangguan, B. Cui, R. Ma et al., *Ceramics International* **42**, 7397 (2016).